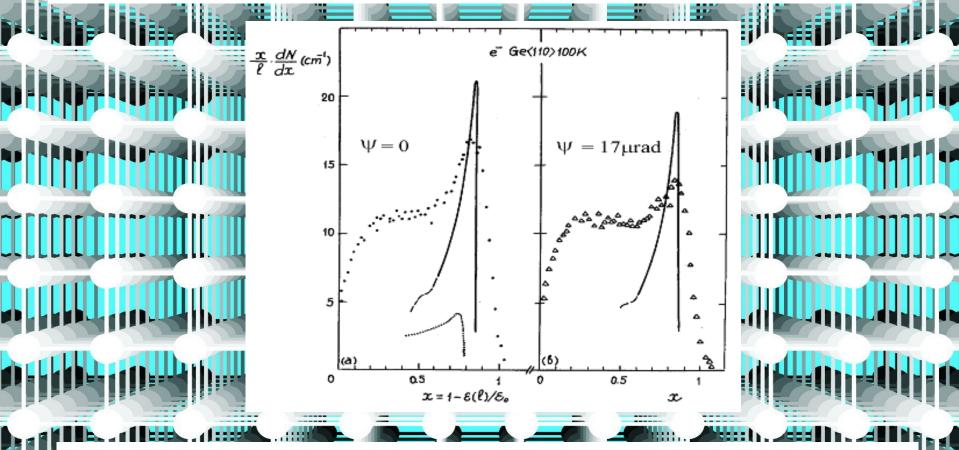


Electron radiative cooling in crystals

Tikhomirov V.V. Phys. Lett. A. 125(1987) 411; NIM B36(1989)282.



Electron radiative loss spectrum expressed in units of electron initial energy **150 GeV** at the angle of incidence Ψ = 0 and 17 μ rad on the Ge crystal plane <110> cooled to 100K. Dotted curve is calculated without taking into account the radiation cooling.

Manifestation of e⁺e⁻ pair production in semi-uniform field crystal field

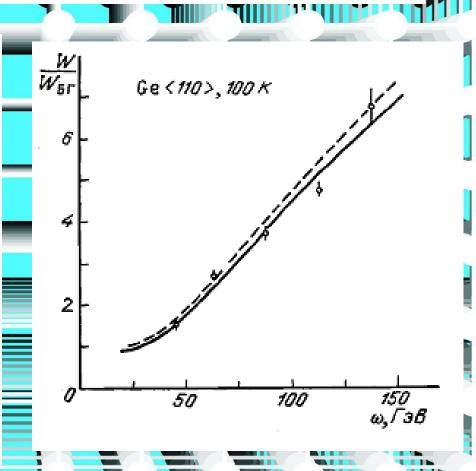
Baryshevskii V.G., Tikhomirov V.V.

Phys. Lett. 90A(1982); Yad. Fiz. 36(1982)697.

Energy dependence of e⁺e⁻ pair production probability by high-energy gamma-quanta

in the field of <110> axes of a Ge crystal at T=100K expressed in units of the Bethe – Heitler probability.

Dots – **experimental data**. The solid and dotted curves are respectively calculated with and without taking into account of the energy dependence of the probability of incoherent PP.



Much more **Strong Field QED** effects will be possible to observe at the **LHC energy**

Positron (electron) anomalous magnetic moment modification influencing spin rotation

V. G. Baryshevsky, Pis'ma Zh. Tekh. Fiz. 5, 182 (1979) [Sov. Tech. Phys. Lett 5, 73 (1979)].

V. G. Baryshevsky and A. O. Grubich, Yad. Fiz. 44, 1114 (1986) [Sov. J. Nucl. Phys. 44, 721 (1986)].

V. V. Tikhomirov, Sov. J. Nucl. Phys. 61, 1188 (1996).

Electron spin rotation in a circularly polarized crystal field harmonics

V. V. Tikhomirov, Pis'ma v Zh. Eksp. Teor. Fiz. 61, 177 (1995).

V. V. Tikhomirov, Phys. Rev. D 53, 7213 (1996).

V. V. Tikhomirov, Sov. J. Nucl. Phys. 62, 664 (1999).

V. V. Tikhomirov, Zh. Eksp. Teor. Fiz. 109, 1188 (1996).

Vacuum dichroism and birefringence

V. G. Baryshevsky and V. V. Tikhomirov, Usp. Fiz. Nauk 159, 529 (1989) [Sov. Phys. Usp 32, 1013 (1989)].

V. G. Baryshevsky and V. V. Tikhomirov, Yad. Fiz. 36, 697 (1982) [Sov. J. Nucl. Phys. 36, 408 (1982)]; Phys. Lett. A 90, 153 (1982).

V. G. Baryshevsky and V. V. Tikhomirov, Nucl. Instr. Meth. A 234, 430 (1985).

V. V. Tikhomirov, Sov. J. Nucl. Phys. 53, 338 (1991).

Electron radiative self-polarization in crystals

V. G. Baryshevsky, A.O. Grubich Pis'ma Zh. Tekh. Fiz. 5, 1529 (1979).

V. V. Tikhomirov, Pis'ma v Zh. Eksp. Teor. Fiz. 58, 168 (1993).

Polarized electron-positron pair production by gamma-quanta

V. G. Baryshevsky and V. V. Tikhomirov, Zh. Eksp. Teor. Fiz. 85, 232 (1983) [Sov. Phys. JETP 58, 135 (1983)]; Phys. Lett. A 96, 215 (1983).

V. G. Baryshevsky and V. V. Tikhomirov, Yad. Fiz. 48, 670 (1988) [Sov. J. Nucl. Phys. 48, 429 (1988)].

Both strong crystal fields and high γ - quantum energies allow to reach the CRITICAL FIELD

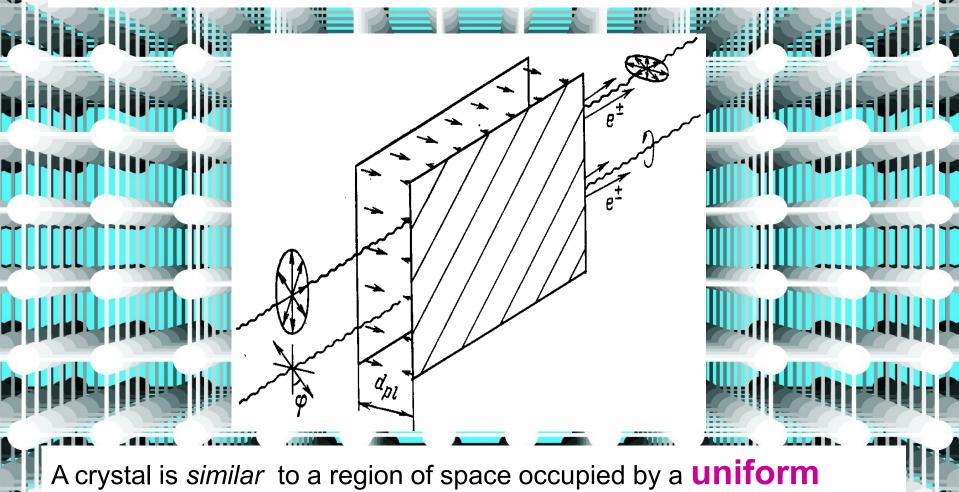
$$E_0 = \frac{m^2 c^3}{e \, \hbar} = 1.32 \cdot 10^{16} \frac{\text{V}}{cm}$$

Table: Maximum electric fields and critical energies for some crystals

Crystal	(plane) or <axis></axis>	$rac{E_{ m max}}{{ m \textit{GV/cm}}}$	$\omega_{th} = \frac{2E_0}{E_{\text{max}}} mc^2$ * TeV
Diamond	(110)	7.7	1.78
	<110>	75	0.20
Si	(110)	5.7	2.39 (1.7)
	<110>	4.6	0.29
Ge	(110)	9.9	1.37 (0.9)
	<110>	78	0.174(0.11)
W	(110)	43	0.316
	<111>	500	0.027

^{*} Electric field reaches E_0 in ref. frame of e^+e^- pair produced at $\omega=\omega_{th}$

The averaged field of crystal planes



A crystal is similar to a region of space occupied by a **uniform** electric field and possesses the properties of **dichroism** and **birefringence** in very hard γ -region

Pair production probabilities by %-quanta polarized along (x) and normal (y) to transverse electric field

$$W_{x,y}(\kappa) = \frac{\alpha m^2}{\sqrt{\pi} \omega^2} \int_0^{\omega} d\varepsilon_+ \left[\int_{\zeta}^{\infty} \Phi(y) dy + \left(2 \pm 1 - \frac{\omega^2}{\varepsilon_+ \varepsilon_-} \right) \frac{\Phi'(\zeta)}{\zeta} \right],$$

$$\Phi(\zeta) = \frac{1}{\sqrt{\pi}} \int_0^{\infty} \cos\left(\zeta t + \frac{t^3}{3} \right) dt, \qquad \zeta = \left(\frac{E_0 m \omega}{E \varepsilon_+ \varepsilon_-} \right)^{2/3}$$

Coherent pair production probabilities by %-quanta polarized along (II) and normal (%) to crystal planes

$$W_{\mathrm{II},\perp}^{coh} = \int_{0}^{d_{\mathrm{g}l}} W_{y,x} \left(\kappa(E(x)) \right) \frac{dx}{d_{\mathrm{g}l}} \,, \qquad \kappa = \frac{E \, \omega}{E_0 \, m}$$

Incoherent pair production probabilities by %-quanta polarized along (II) and normal (Υ) to crystal planes

$$W_{\text{II}(1)}^{inc} = \frac{1}{15L_{rad}\omega^3} \int_0^{d_{pl}} \frac{n(x)}{n_0} \frac{dx}{d_{pl}} \int_0^{\omega} d\varepsilon_+ \left[1 - \theta(1 - \zeta) \frac{\ln \zeta}{2\ln(183Z^{-1/3})}\right] \times$$

$$\begin{split} &+ (\mathcal{E}_{+}^{2} + \mathcal{E}_{-}^{2})[(1 \mp 1)\zeta^{4}Y + (3 \pm 6)\zeta Y - (5 \mp 4)\zeta^{2}Y' - (1 \mp 1)\zeta^{3}]], \\ & Y = Y(\zeta) = \int_{2}^{\infty} \sin\left(\zeta t + \frac{t^{3}}{3}\right), \end{split}$$

$$n(x) = \frac{n_0 d_{pl}}{\sqrt{2\pi u}} \exp\left(-\frac{x^2}{2u^2}\right), \qquad \frac{1}{L_{rad}} = 4\alpha n_0 \left(\frac{Z\alpha}{m}\right)^2 \ln(183 Z^{-1/3})$$

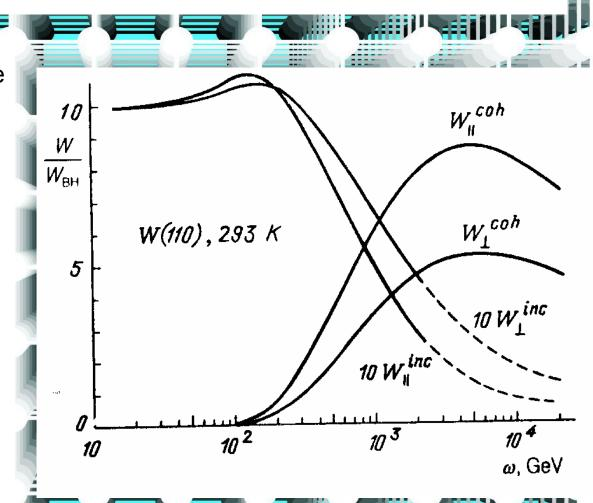
Total pair production probabilities by polarized %-quanta in crystals $W_{\mathrm{II}(\perp)} = W_{\mathrm{II}(\perp)}^{coh} + W_{\mathrm{II}(\perp)}^{inc}$ Pair production asymmetry $W_{\Pi}-W_{\perp}$ $W_{
m II} + W_{
m L}$

Synchrotron-like crystal dichroism

Energy dependence of the coherent and incoherent contributions to the probability of

e⁺e⁻ pair production

by γ -quanta **polarized** parallel and normal to the <110> planes of tungsten, along which these γ - quanta are propagating.



Dichroic crystal polarizer

Optimal

polarizator length

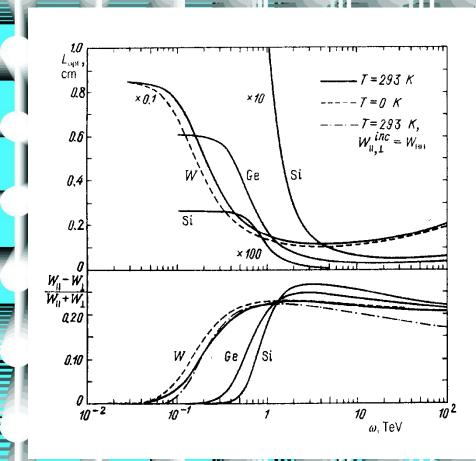
and

pair production asymmetry

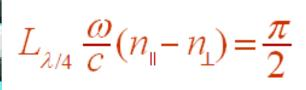
for <110> planes of crystals of Si,Ge and W at T=293K (below).

Dotted curves - for W at T=0K, dot-dash – also for W, but

neglecting the energy and polarization dependence of the incoherent contribution of PP at T=293K.



Synchrotron-like crystal birefringence

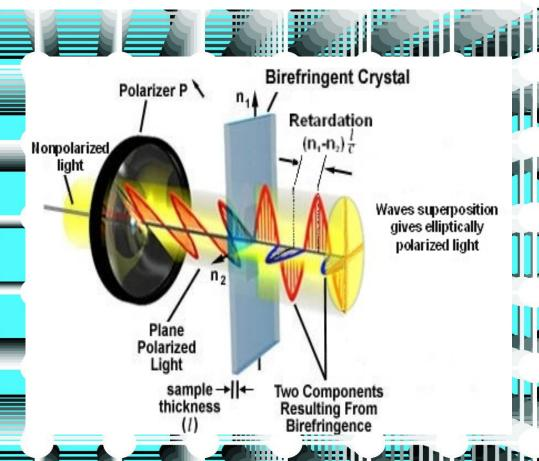


For visible light

$$\Delta t = 10^{-15} \mathrm{s}$$

For γ - quanta

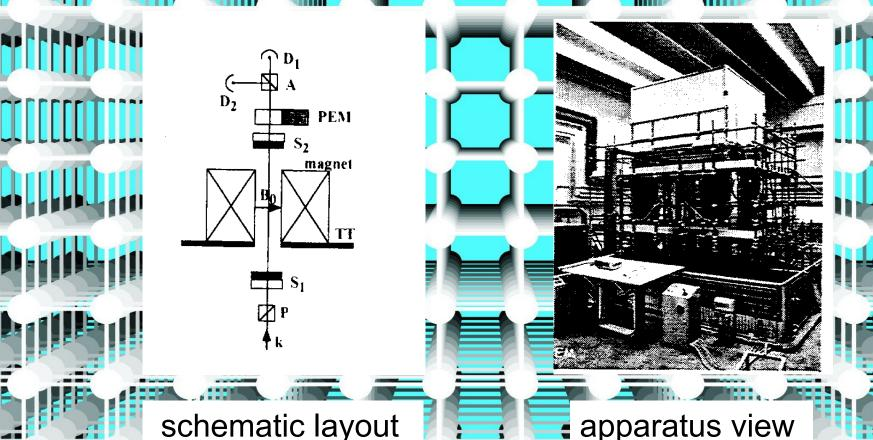
$$\Delta t = 10^{-28} \text{s}$$



- determines polarization of Neutron Star gamma radiation
- is experimentally searched for a long time

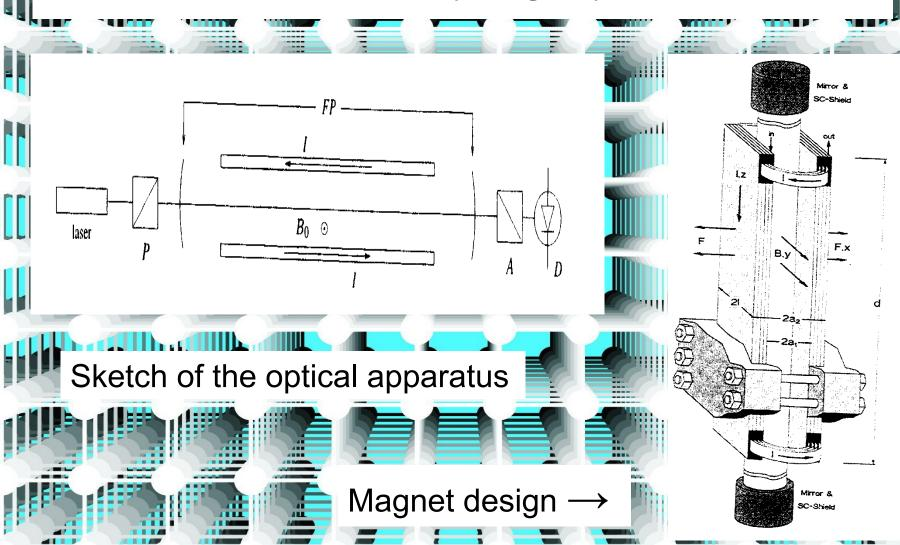


Polarizzazione del Vuoto con LASer (PVLAS) Laboratori Nazionali di Legbaro of INFN, Padova



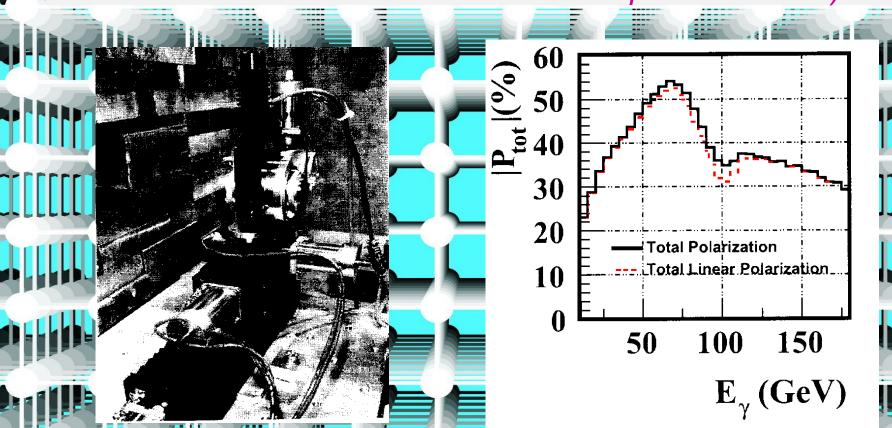


Laboratoire National das Champs Magnetique Pulses, Toulouse



Crystal birefringerence (Cabibbo, 1962)

CERN (Armenia-Sweden-Italy-Switzerland-USA-South Africa-France-Netherlands-Russia-Spain-Danmark)



Birefringent (quarter wave plate) Si crystal and goniometer

Stokes parameters after the quarter wave crystal

Refraction indexes of %-quanta polarized along (II) and normal (Υ) to crystal planes

$$n_{\Pi(\perp)} = n_{\Pi(\perp)}^{coh} + n_{\Pi(\perp)}^{inc}$$

$$n_{\Pi(\perp)}^{coh}(\omega) = \int_{0}^{d_{pl}} n_{y(x)}(K(x)) \frac{dx}{d_{pl}}$$

$$n_{x(y)}(K) = \frac{1}{2} \Re \varepsilon_{x(y)} = 1 - \frac{\alpha}{3\pi} \left(\frac{E}{\kappa E_{0}}\right)_{0}^{2} \frac{Y'(\zeta)}{\zeta} \left(\frac{\omega^{2}}{\varepsilon_{+}\varepsilon_{-}} + \frac{1\mp 3}{2}\right) \frac{d\varepsilon_{+}}{\omega}$$

$$n_{\Pi(\perp)}^{inc} = n_{\omega <<\omega_{\kappa-1}} - \frac{\sqrt{\pi}}{30 L_{rad}} \int_{0}^{d_{pl}} \frac{n(x)}{n_{0}} \frac{dx}{d_{pl}} \times \frac{1}{2} \left(\frac{\omega^{2}}{\varepsilon_{+}\varepsilon_{-}} + \frac{1\mp 3}{2}\right) \frac{d\varepsilon_{+}}{\omega}$$

$$\times \int_{0}^{\omega} d\varepsilon_{+} \left(\omega^{2} \left[(1\pm 1)\zeta^{4}\Phi \mp 6\zeta\Phi - (3\pm 4)\zeta^{2}\Phi'\right] + (\varepsilon_{+}^{2} + \varepsilon_{-}^{2})\left[(1\mp 1)\zeta^{4}\Phi + (3\pm 6)\zeta\Phi - (5\mp 4)\zeta^{2}\Phi'\right]\right)$$

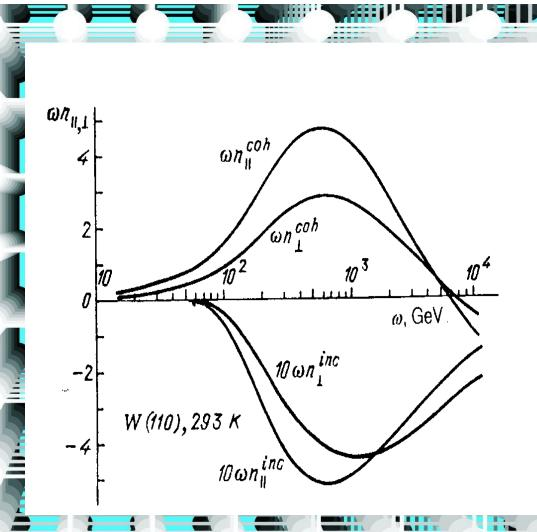
1 1 1 1 1 1

The LHC energy is really optimal:

multiplied by energy coherent and incoherent contributions to the

refractive indexes

of γ -quanta linearly polarized parallel and perpendicular to the <110> planes of a tungsten crystal at T=293K.

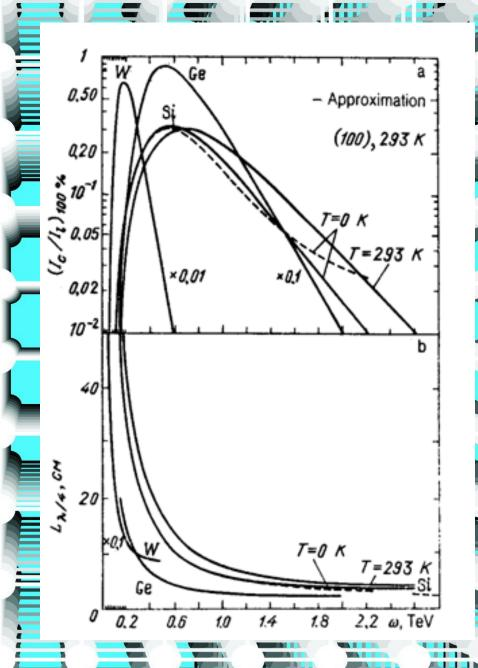


Energy dependence of attenuation coefficients of a completely polarized beam and lengths of

quarter-wave plates

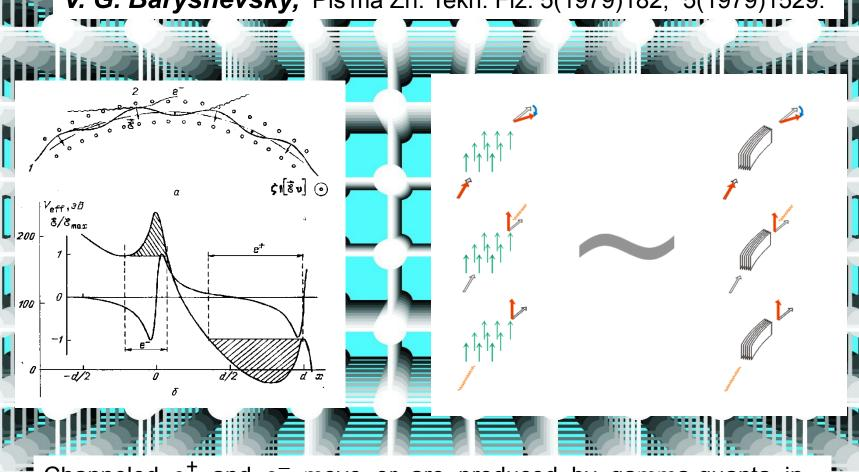
based on using the birefringence property of the fields of the <110> planes of Ge and W crystals at T=293K, and also Si at 0 and 293K

Dotted curves are calculated by using the simplified description of the refraction and the absorption by the Bethe – Heitler probability.



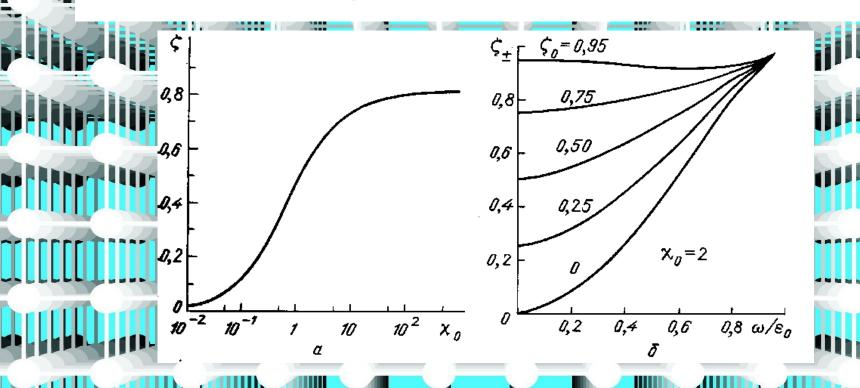
Spin effects in bent crystal

V. G. Baryshevsky, Pis'ma Zh. Tekh. Fiz. 5(1979)182; 5(1979)1529.



Channeled e⁺ and e⁻ move or are produced by gamma-quanta in bent crystals in the regions with dominating direction of the planar electric field, which represents itself an origin of a number of spin effects.

Radiative self-polarization in the uniform field



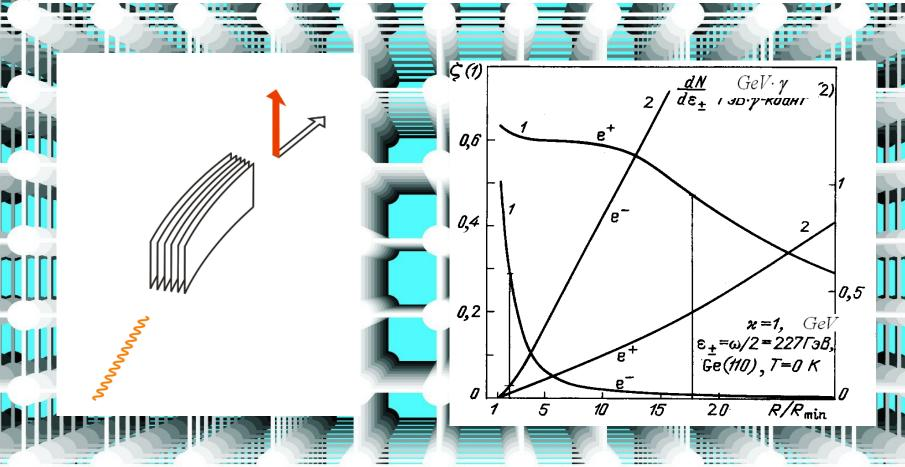
Maximal polarization attained by e^{\pm} losing all their energy for radiation the initial value of the χ .

Final e^{\pm} polarization vs the energy of emitted γ -quantum at different initial polarizations and $\chi_0 = 2$.

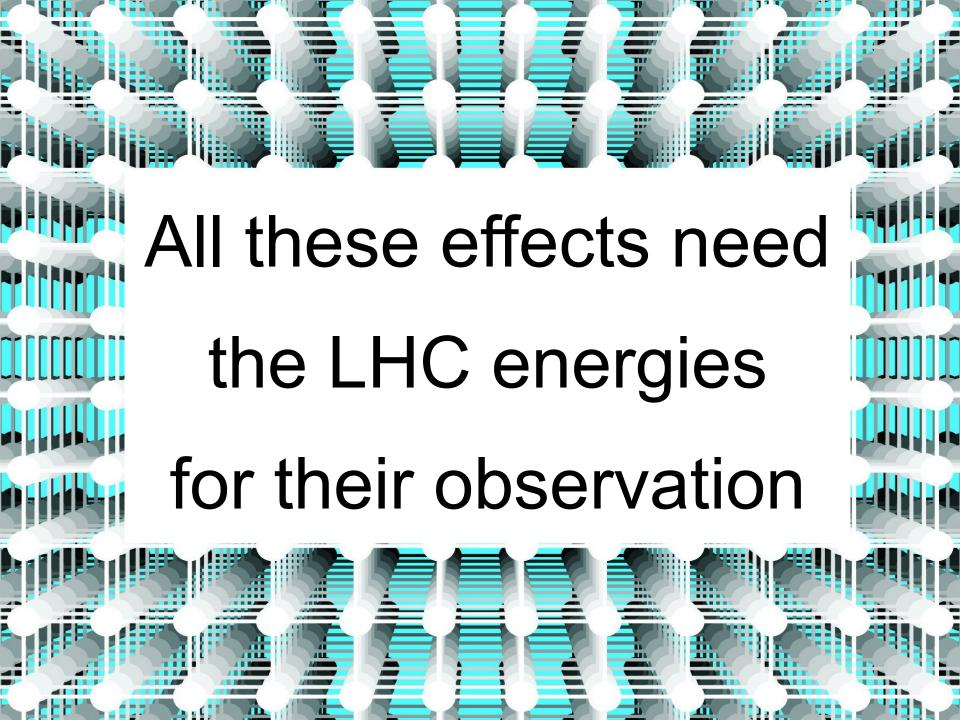
$$\chi = \frac{E}{1.32.10^{16} \text{ eV/cm}} \frac{\mathcal{E}}{\text{me}^2}$$
 - the main parameter of quantum electrodynamics

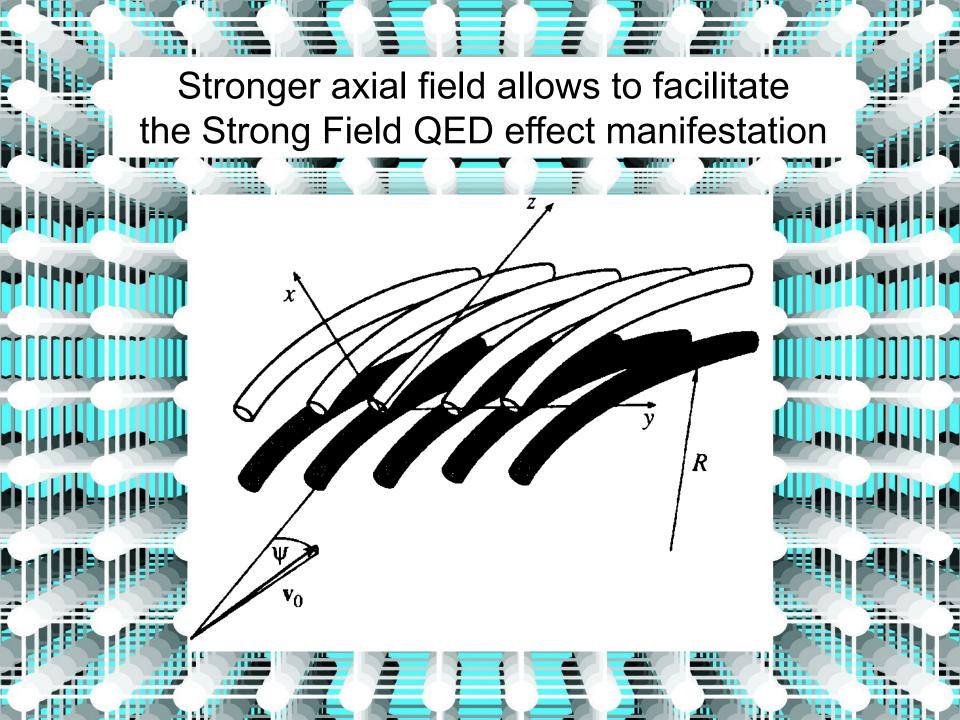
Radiative self-polarization in bent crystals at purely planar channeling 0.2 -0.20.8 0.4 x = E/E-0.8 FIGURE 1 Polarization (curves 1 and 2) and energy distribution (curves 3 and 4) gained by positrons 0.2 with initial energy $E_0 = \frac{287 \text{ GeV}}{E_0}$ in the bent $\frac{E_0}{E_0}$ in the bent $\frac{E_0}{E$ the crystal of length l = 1 cm. FIGURE 2 Electron and positron polarization gained in Si(110) crystal at $T = 293 \, \text{K}$ versus fina energy, expressed in units of initial energy $E_0 = \frac{1}{2} \text{TeV}$. Curves 1 and 2—for electrons, 3 and 4—for positrons. Curves 1 and 3—for constant radius $R = 5.3 \,\text{m}$ of crystal bent, curves 2 and 4—for crystal

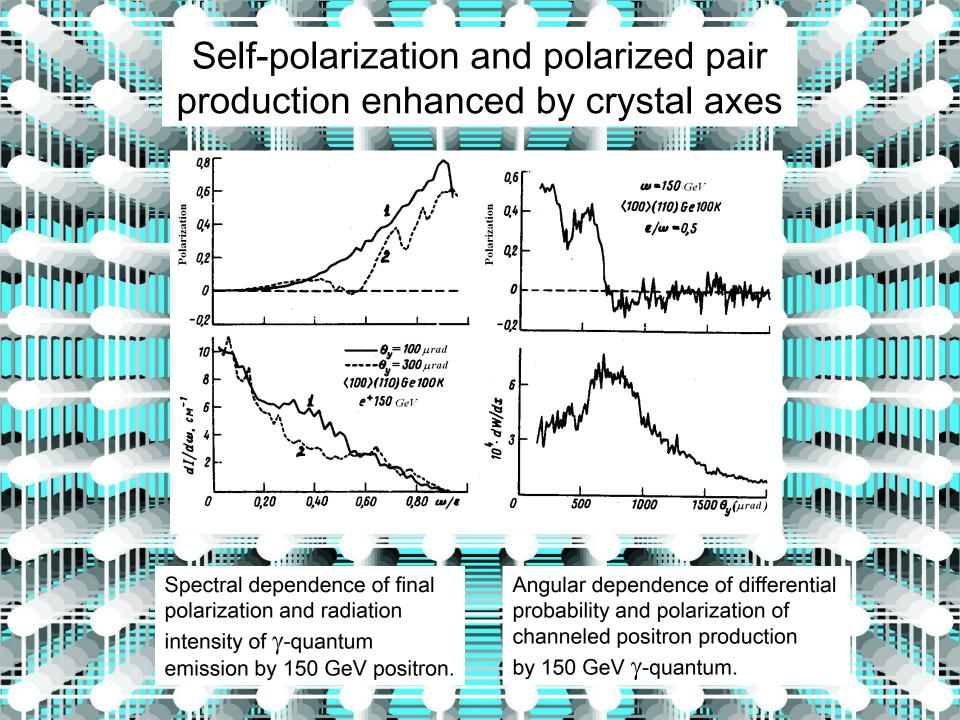




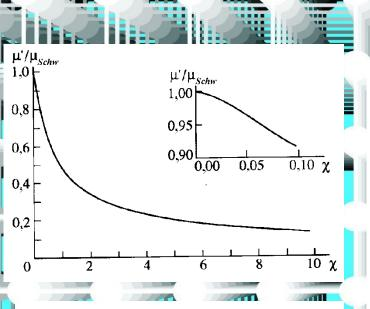
Differential number and polarization of e^{\pm} , produced with energy of 227 GeV vs the Ge(110), T = 0K, crystal bending radius. Vertical lines indicate the optimal bending radius values.



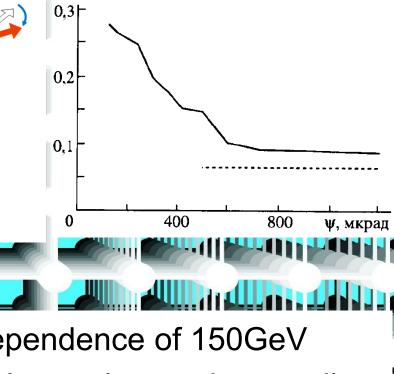




Positron magnetic moment modification

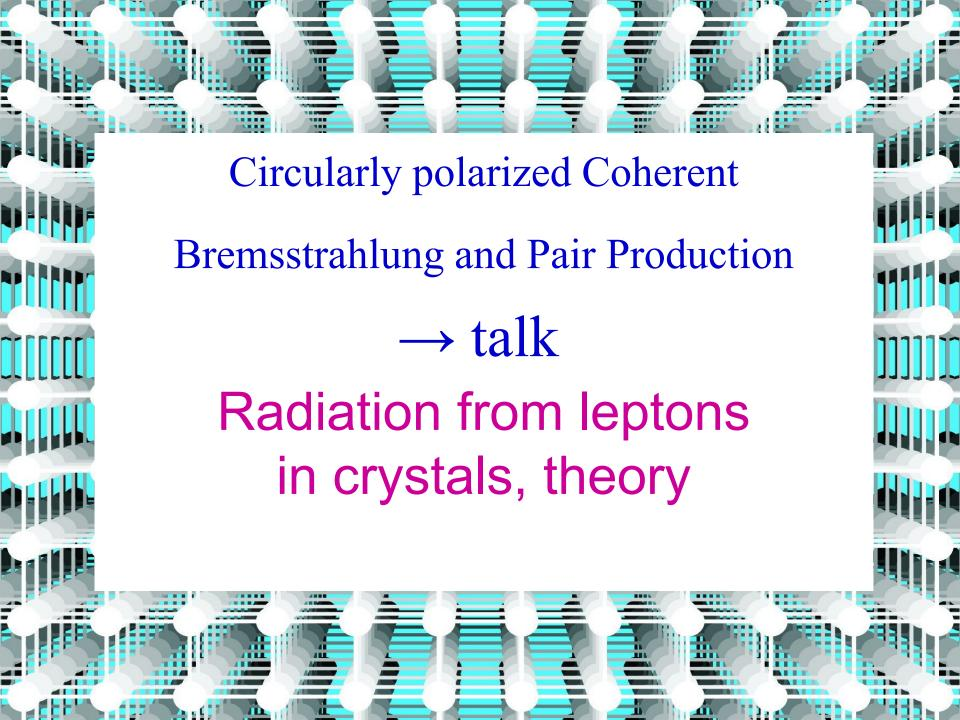


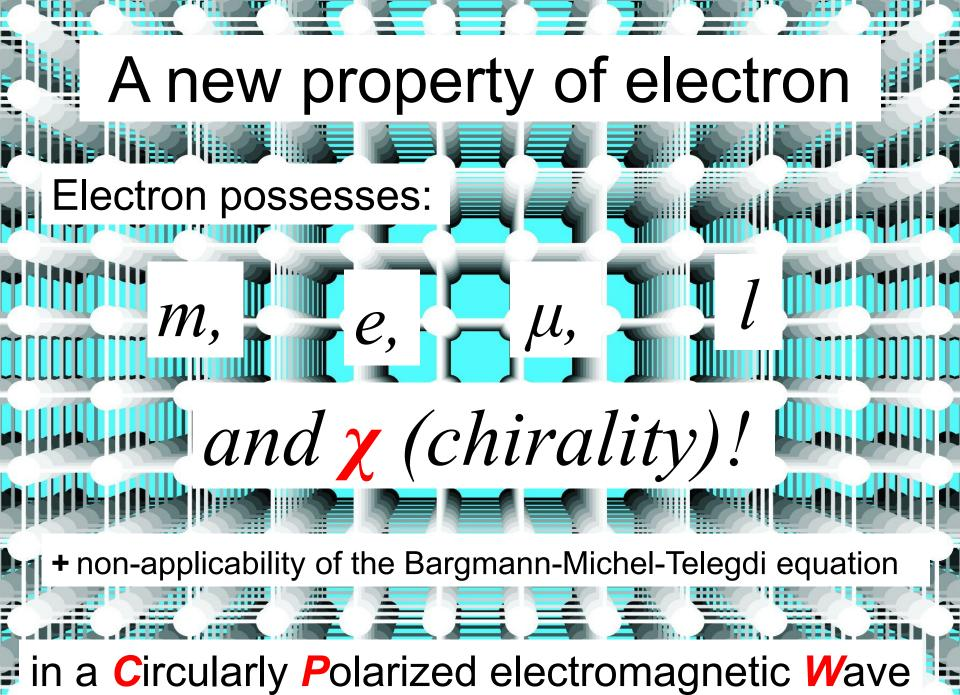
Anomalous magnetic moment dependence on $\chi = E'/E_0$ in the uniform field, $\mu_{Schw} = (\alpha/2\pi)\mu_0$.

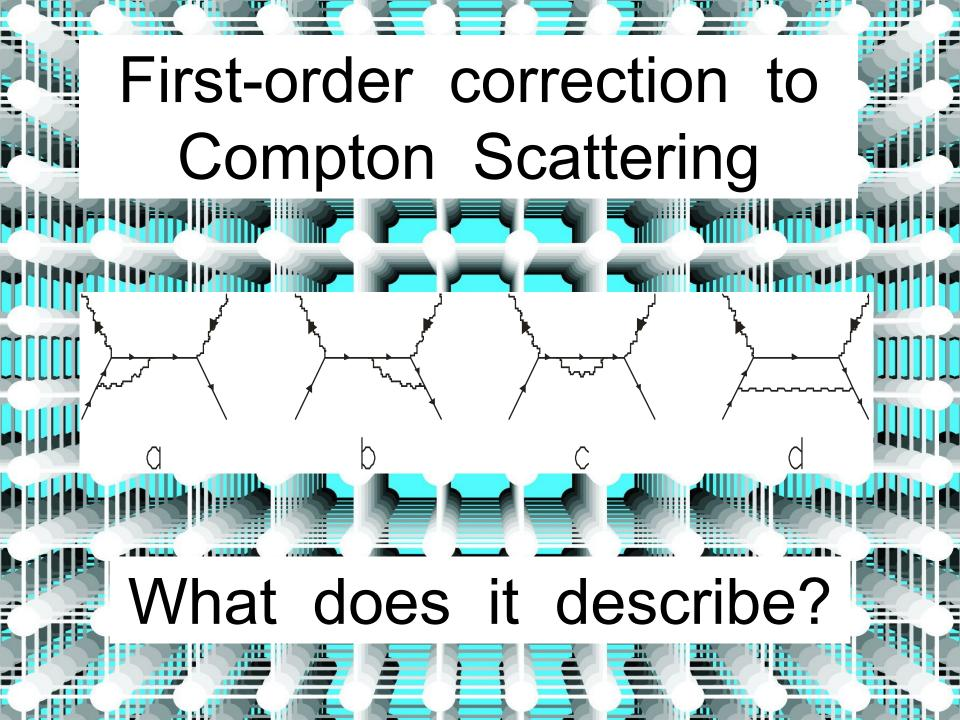


Angular dependence of 150GeV positron spin rotation angle revealing its magnetic moment modification.

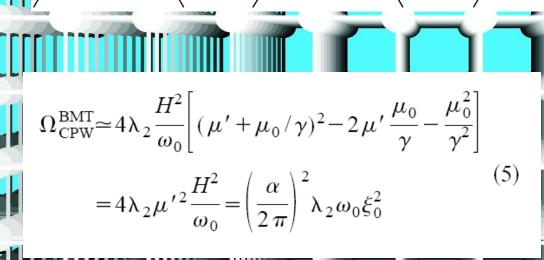
–∆ф, рад/мм







Magnetic moment precession in a CPW



Corresponds to the predictions of Bargmann-Michel-Telegdi equation

 $\Omega^{(3)} = \left(\frac{\alpha}{2\pi}\right)^2 \lambda_2 \omega_0 \xi_0^2 \qquad (24)$

Chirality manifestation in a CPW

$$\Omega^{(2)} = -\frac{2H^2}{\varepsilon\omega_0}\lambda_2 f_2^{(2)}(\varepsilon) = -\frac{mH^2}{\varepsilon\omega_0^2}\lambda_2 f_2^{(2)}(\omega)$$

$$= \frac{\alpha}{\pi}\lambda_2\omega_0\xi_0^2 \frac{1}{x} \left\{ \left(\frac{2}{x} - 1\right) \left[F(x - 1) + \frac{\pi^2}{6} \right] - \left(\frac{2}{x} + 1\right) [F(x) - \ln x \ln(1 + x)] + \frac{x}{1 - x^2} + \frac{2x^3 \ln x}{(1 - x^2)^2} \right\}$$
(25)

Does not correspond to the predictions of the Bargmann-Michel-Telegdi equation!

 $x \approx 4\varepsilon \omega_0/m^2 \approx 0.0153\varepsilon (\text{GeV})\omega_0(\text{eV}) \approx 0.019\varepsilon (\text{GeV})/\lambda(\mu\text{m}).$

Chirality can be easily observed both in laser field and bent crystal

Chirality can be observed both in a laser field and bent crystal

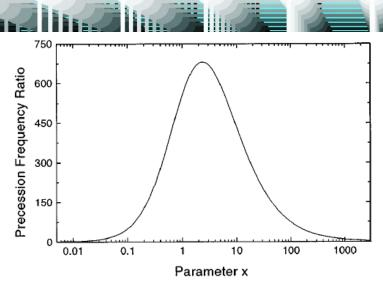


FIG. 2. The dependence on the parameter x of the ratio $R = -\Omega^{(2)}/\Omega^{(3)}$ of the contribution (25) of order α^2 to the electron spin precession frequency in a CPW in the limit of $\xi_0^2 \ll 1$, to the contribution (24) of order α^3 equal to the spin precession frequency (5), following from the BMT equation.

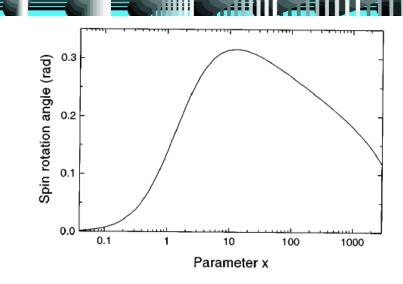


FIG. 3. The dependence on the parameter x of the rotation angle of transverse electron spin component in a CPW on a typical length of the inverse Compton scattering in the limit $\xi_0^2 \ll 1$ of nonrelativistic transverse electron motion.

$$x \simeq 4\varepsilon \omega_0 / m^2 \simeq 0.0153\varepsilon (\text{GeV}) \omega_0 (\text{eV}) \simeq 0.019\varepsilon (\text{GeV}) / \lambda (\mu \text{m}).$$

What is suggested to observe:

e⁺e⁻ pair production in semi-uniform field crystal field Electron radiative cooling

Strong Field QED effects observable only at the **LHC energy**:

Synchrotron-like (uniform field) dichroism and birefringence in very hard γ -region

Spin effects in bent crystal:

Radiative *self-polarization* in bent crystals
Production of transversely *polarized e*[±]
by γ-quanta in bent crystals
Positron *magnetic moment modification*

Circularly polarized Coherent Bremsstrahlung and Pair Production.

Allow to generate:

circularly polarized gamma-quanta, longitudinally polarized positrons, longitudinally polarized *electrons*.

Allow to measure:

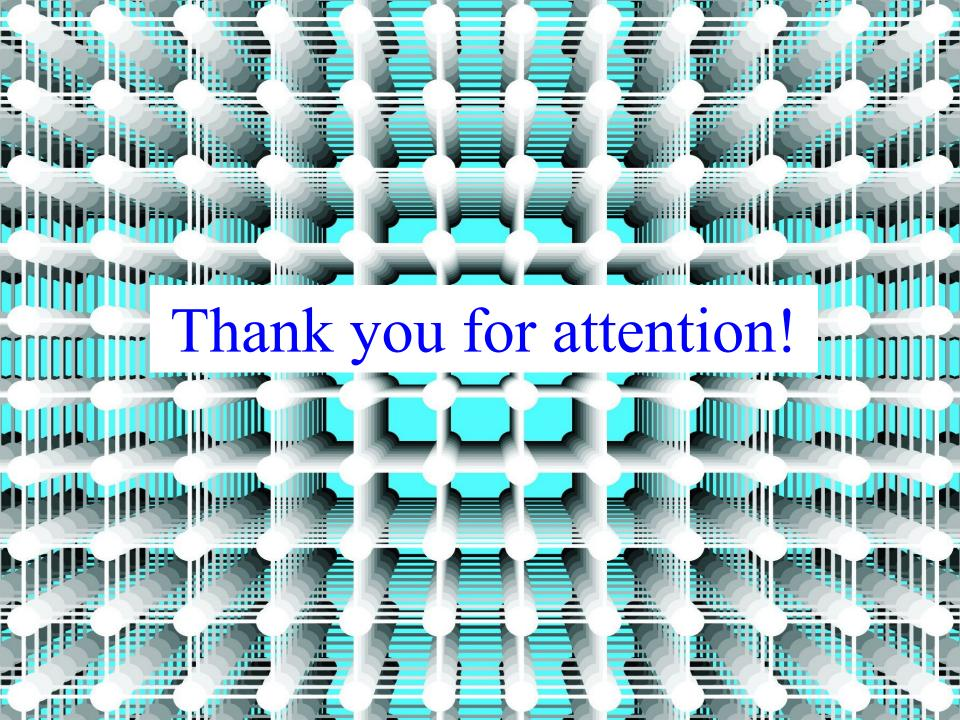
gamma circular polarization, longitudinal positron polarization.

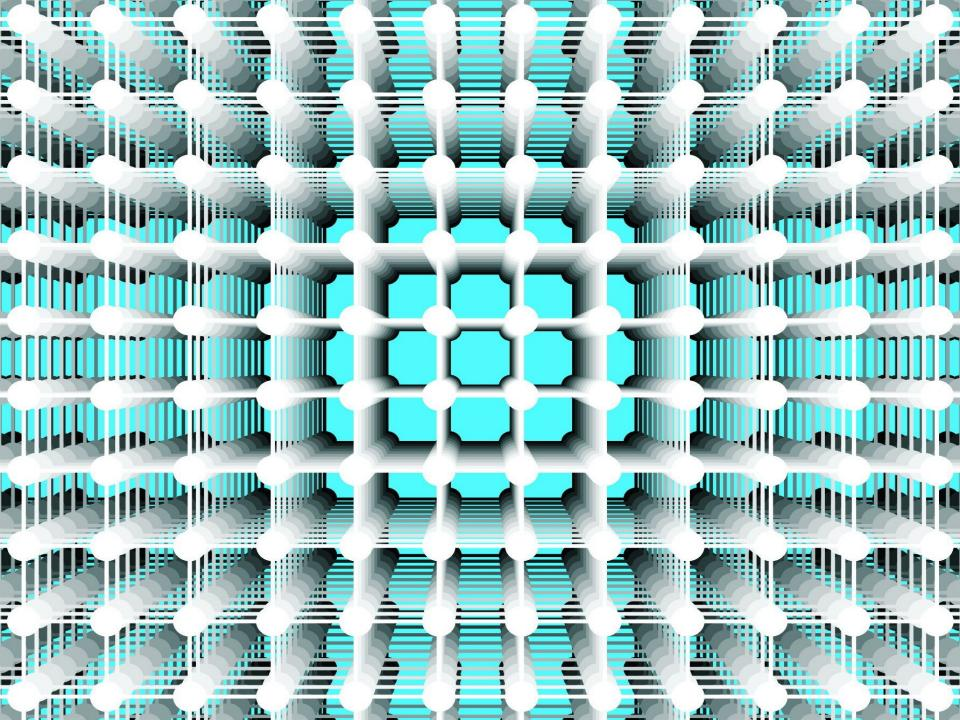
Chirality, a new property of electron

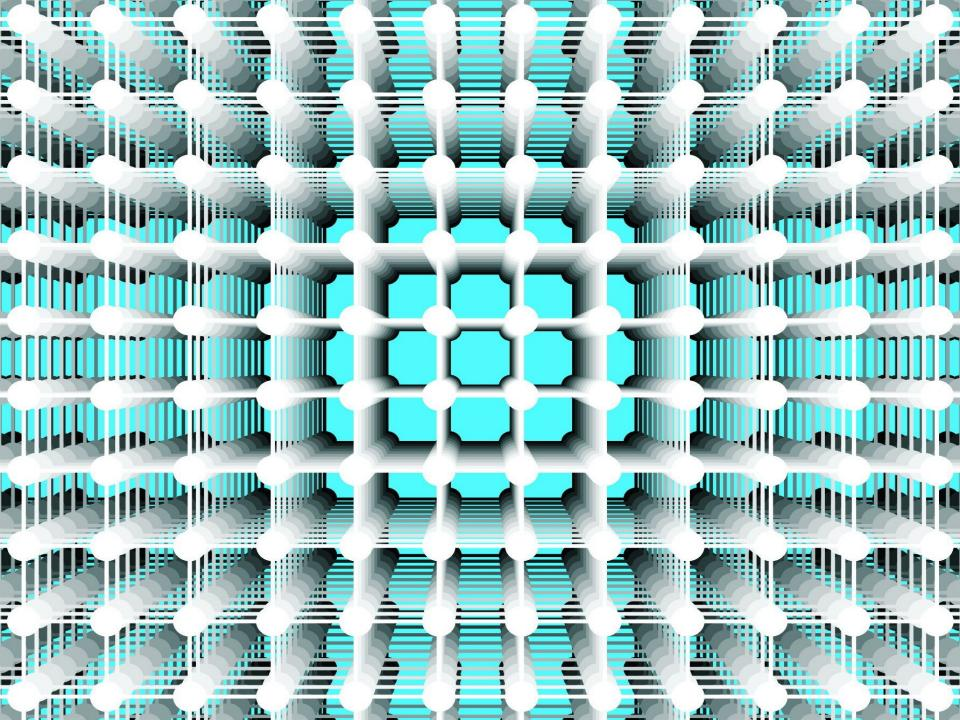
Can be observed in both laser field and bent crystals.

Radiation in MVROC conditions.

Incoherent radiation suppression by crystal cut...







Both strong crystal fields and high γ - quantum energies allow to reach the CRITICAL FIELD

$$E_0 = \frac{m^2 c^3}{e \, \hbar} = 1.32 \cdot 10^{16} \frac{\text{V}}{cm}$$

Table: Maximum electric fields and critical energies for some crystals

Crystal	(plane) or <axis></axis>	$rac{E_{ m max}}{{ m \textit{GV/cm}}}$	$\omega_{th} = \frac{2E_0}{E_{\text{max}}} mc^2$ * TeV
Diamond	(110)	7.7	1.78
	<110>	75	0.20
Si	(110)	5.7	2.39 (1.7)
	<110>	4.6	0.29
Ge	(110)	9.9	1.37 (0.9)
	<110>	78	0.174(0.11)
W	(110)	43	0.316
	<111>	500	0.027

^{*} Electric field reaches E_0 in ref. frame of e^+e^- pair produced at $\omega=\omega_{th}$



LHC opens up the possibilities to observe the strong field QCD effect of uniform field dichroism and birefringence in crystals in optimal energy region

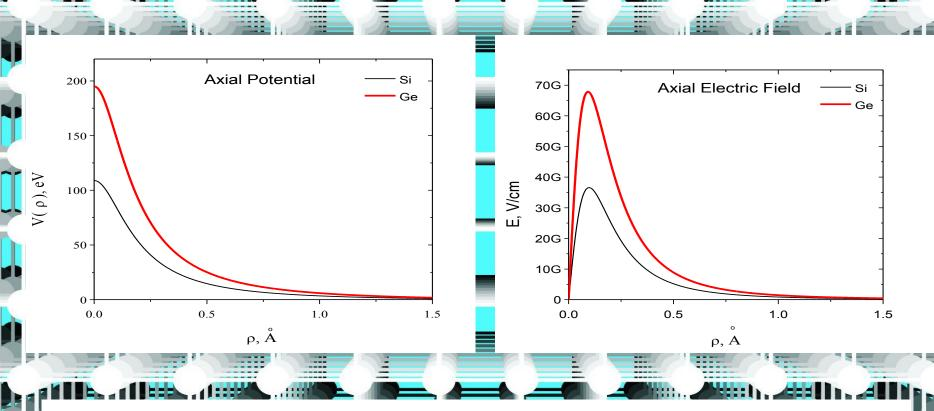
Also can be observed:

Strong electron magnetic moment modification Production of polarized electrons and positrons Electron radiative self-polarization

Outline

- Coherent bremmstrahlung and its linear polarization
- •String-of-strings crystal orientation
- Polarization of crystal field harmonics
 - Circular polarization of radiation of positrons channeled in bent crystals with string-of-strings orientation
 - Polarization asymmetry of channeled positron production
 - Other manifestations of circular polarization of the crystal field harmonic
 - Conclusions

Comparison of axial potential and field strength in Si and Ge



Both potential and field strength are nearly twice as larger in Si than in Ge

Comparison averaged potentials and field strengths of Ge and Si planes and axes

		Si(293K)	Ge(293K)		Ge(100K)	
<110>	V ₀ , eV	133	229	172%	309	232%
<110>	E _{max} ,GV/cm	46	78	170%	144	313%
		Si(293K)	Ge(293K)		Ge(0K)	
(110)	V ₀ , eV	21.5	37.7	175%	44.0	205%
(110)	E _{max} ,GV/cm	5.7	9.9	1.74	14.9	261%

u(293K)=0.085Å, u(100K)=0.054Å, u(0K)=0.036Å

Ge cooling is very productive!

Investigating Strong Field QED effects

$$\chi = \frac{E}{1.32 \cdot 10^{16} eV/cm} \frac{\mathcal{E}}{mc^2}$$
 - the main parameter of quantum electrodynamics

		Si(293K)	Ge(293K)		Ge(100K)	
<110>	E _{max} ,GV/cm	46	78	170%	144	313%
	χ(120GeV)	0.82	1.39		2.56	

 $I(\chi \ll 1) \propto E^2$,

 $I(\chi \sim 1) \propto E$,

 $I(\chi >> 1) \propto E^{2/3}$

Radiation intensity will grow like $E \div E^2$